A combined numerical and experimental investigation of disengaged wet brake plate power loss

A Combined Numerical and Experimental Investigation of Disengaged Wet Brake Plate Power Loss

M. Leighton[1*], N. Morris[1], R. Rahmani[1], G. Trimmer[2], P.D. King[1] and H. Rahnejat[1]

[1] Wolfson School of Mechanical and Manufacturing Engineering, Loughborough University, Leicestershire, UK

[2] J.C. Bamford Excavators, Rocester, Staffordshire, UK

[*] Corresponding author: M.Leighton@lboro.ac.uk

Abstract

Increased machine performance through reduction of drivetrain power losses is an important goal in powertrain engineering. One key area of power loss in the driven axles of heavy on-road vehicles and off-highway vehicles is the disengaged wet brake conjunctions. The resultant power loss, particularly under cold start conditions, can be quite significant. The addition of patterned grooves into the brake friction linings assists lubricant flow to dissipate heat during contact, which complicates the prediction of performance, making design improvement a multi-variate problem. A Reynolds-based numerical model with the inclusion of lubricant inertial terms is developed, allowing time efficient prediction of the conjunctional torsional viscous losses. The numerical model is validated with CFD as well as experimental measurements, using a developed component based test rig. Good agreement is found for predictions against measurements for lower viscosity lubricant flow at higher bulk oil temperatures. The results show deviations at lower temperatures promoting higher viscosity inlet starvation, which is not taken into account with the assumed fully flooded inlet.

Keywords: *Wet grooved brake plates, Power loss, Efficiency, Micro-hydrodynamics*

1 - Introduction

Reduction of power losses, leading to improved system efficiency, thus reduced harmful emissions is the key objective of modern powertrain engineering. There is progressive stringent emissions legislation and directives on emission levels and customer driven demands for

improved fuel efficiency and machine reliability. These pressures are brought upon both on- and off-highway vehicle manufacturers.

With regard to off-highway as well as heavy vehicles, a key area of power loss is friction and drag of wet multi-plate brakes. In particular, power loss under disengaged conditions has been found to be significant, where improvements can potentially be made. These components can, by their design, result in periods of operation where there can be significant relative rotational velocities of plates with only a thin lubricant film separating them. The resultant power loss, particularly under cold start conditions, can be quite significant. The addition of patterned grooves into the brake friction linings, to allow oil flow to dissipate heat during contact complicates the prediction of performance, making the design improvement a multi-variate problem.

A time efficient predictive method for torsional losses associated with various wet brake friction plate designs is required to analyse and compare the effect of different fabricated patterns. The application of Computational Fluid Dynamics (CFD) to model various pattern designs is considered to be quite time consuming, as each change in operational geometry requires a re-meshing of the simulated domain.

2 - Method

Modelling of hydrodynamic flow in simple, micro-scale or larger gaps is usually performed by either analytical solutions, where the geometry and fluid flow allow, or by computation fluid dynamics (CFD). CFD is a far more complex approach than it may initially appear and although it is relatively easy to obtain predictions there is no simple way of verifying their validity. Furthermore, any change in design through a multitude of factors, particularly geometry would require time consuming and complex remeshing of the domain.

A far simpler solution for modelling full film hydrodynamics is the use of Reynolds equation as a simplification to the more general Navier-Stokes equation in the CFD approach. Reynolds equation makes the assumption that there is pressure gradient into the depth of a lubricant film (i.e. in the z direction) and the flow within the contact remains laminar of a single phase. Therefore, there is no need to have nodal positions between the surfaces into the depth of a

lubricant film. A mesh can therefore be considered as a simple array, mapped onto the modelled contact area. Reynolds equation in its simplified form (in polar coordinate systems) becomes:

$$\frac{\partial}{\partial c}\left(\frac{h^3}{12\eta}\frac{\partial p}{\partial c}\right)+\frac{\partial}{\partial r}\left(\frac{h^3}{12\eta}\frac{\partial p}{\partial r}\right)=\frac{U_1+U_2}{2}\frac{\partial h}{\partial c}+\frac{\partial h}{\partial t} \quad (1)$$

where r denotes the radial direction, c denotes the circumferential direction, h is the local film thickness, p is the generated hydrodynamic pressure, η is the lubricant dynamic viscosity and U is the speed of entraining motion of the lubricant into the contact. The form of Reynolds equation stated above assumes no side leakage flow in the radial direction of the contact of a pair of brake discs. For all the assumptions underlying Reynolds equation see [1-3].

Another assumption of the above formulation is that there is no inertial effect due to body forces as the lubricant film is considered to be quite thin and the laminar flow is under steady state conditions. In some applications this assumption may not quite hold, for example for a rotating brake there is an acceleration associated with centripetal force which should normally be considered. Inclusion of the inertial terms in the Reynolds equation results in a considerable increase in the time required for a numerical solution. Reynolds equation with inclusion of inertial terms becomes:

$$\begin{aligned}\frac{\partial}{\partial c}\left(h^3\frac{\partial p}{\partial c}\right)+\frac{\partial}{\partial r}\left(h^3\frac{\partial p}{\partial r}\right)-6\eta(U_1+U_2)\frac{\partial h}{\partial c}-12\eta\frac{\partial h}{\partial t}\\ =-2\rho h\frac{\partial h}{\partial c}\left(\frac{\partial I^{cc}}{\partial c}+\frac{\partial I^{cr}}{\partial r}\right)-2\rho h\frac{\partial h}{\partial r}\left(\frac{\partial I^{cr}}{\partial c}+\frac{\partial I^{rr}}{\partial r}\right)\\ -\rho h^2\left(\frac{\partial^2 I^{cc}}{\partial c^2}+2\frac{\partial^2 I^{cr}}{\partial c\partial r}+\frac{\partial^2 I^{rr}}{\partial r^2}-\frac{\partial^2 h}{\partial t^2}\right)-12h\left(U_1\frac{\partial \eta}{\partial c}+W_1\frac{\partial \eta}{\partial r}\right)\\ +2h\left[\frac{\partial h}{\partial c}(\tau_{ph}^{c\alpha}-\tau_{p0}^{c\alpha})+\frac{\partial h}{\partial r}(\tau_{ph}^{\alpha r}-\tau_{ph}^{\alpha r})\right]+h^2\left[\frac{\partial}{\partial c}(\tau_{ph}^{cr}-\tau_{p0}^{cr})+\frac{\partial}{\partial r}(\tau_{ph}^{\alpha r}-\tau_{ph}^{\alpha r})\right]\end{aligned} \quad (2)$$

where, ρ is the lubricant density, I is the inertial effect and τ is the shear stress.

3 - Numerical Model

The developed numerical model in the current study includes a discretised Reynolds equation with inertial terms to the case of measured brake disc geometry. Convergence of predicted pressure loops is sought, such that the error between successive iterations is decreased by 3 orders of magnitude from an initial guess. Gauss-Seidel point successive over relaxation iterative

method is used. The resulting pressure distribution is then used to determine the contribution of pressure driven flow in generating power loss and coupled with the lubricant shear contribution. Cavitated regions of flow are considered to have no pressure gradient and lubricant transport is determined through conservation of mass from the cavitation boundary.

In order to allow for comparisons of different brake patterns, it is necessary to consider other factors of importance in the numerical model. As a result the total contact area of any pattern is considered together with its mean effective radius. These parameters are considered to be representative of the performance of the brake disc pattern to operate as intended, when engaged. Furthermore, the lubricant flow rate at the outer radius of the disc is modelled and recorded as this is considered to be proportional to the lubricant flow across the plates via the surface groove feature when the component plates are engaged.

4 – The CFD Model

A CFD analysis is also undertaken in addition to the finite difference Reynolds based method as a partial validation of the latter. The same CAD geometry is used as a nodal film thickness input into the above described numerical model as the basis of the CFD analysis in order to ensure identical conditions between the CFD analysis and the Reynolds-based approach.

The CFD analysis uses a periodic boundary condition at the repeating edges of the computational domain in order to reduce the computational times. A pressure inlet boundary condition is applied at the internal edge of the domain and at the pressure outlet, set at the external radii of the discs. The boundary conditions are shown in Figure 1 and are in-line with similar studies [4, 5].

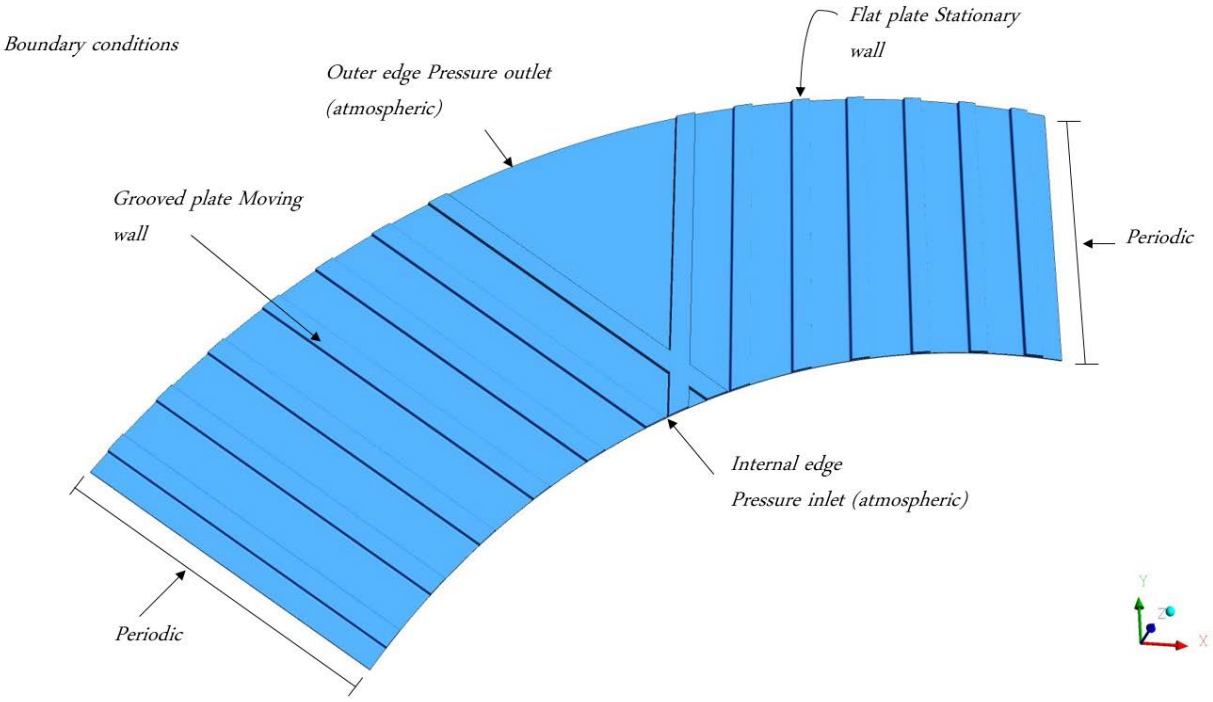

Figure 1: Boundary conditions for the CFD analysis of the brake disc geometry

The modelled brake geometry is used in the CFD model with the operational conditions listed in Table 1.

Table 1: Model input parameters

Inner Diameter	160 mm
Outer Diameter	220 mm
Rotation speed	926 rpm
Minimum Separation	180 µm
Lubricant Dynamic Viscosity	10.6 cP (at 100°C)
Lubricant Density	880 kgm^{-3} (at 100°C)

The pressure distribution over the brake geometry, predicted through CFD analysis can be seen in Figure 2.

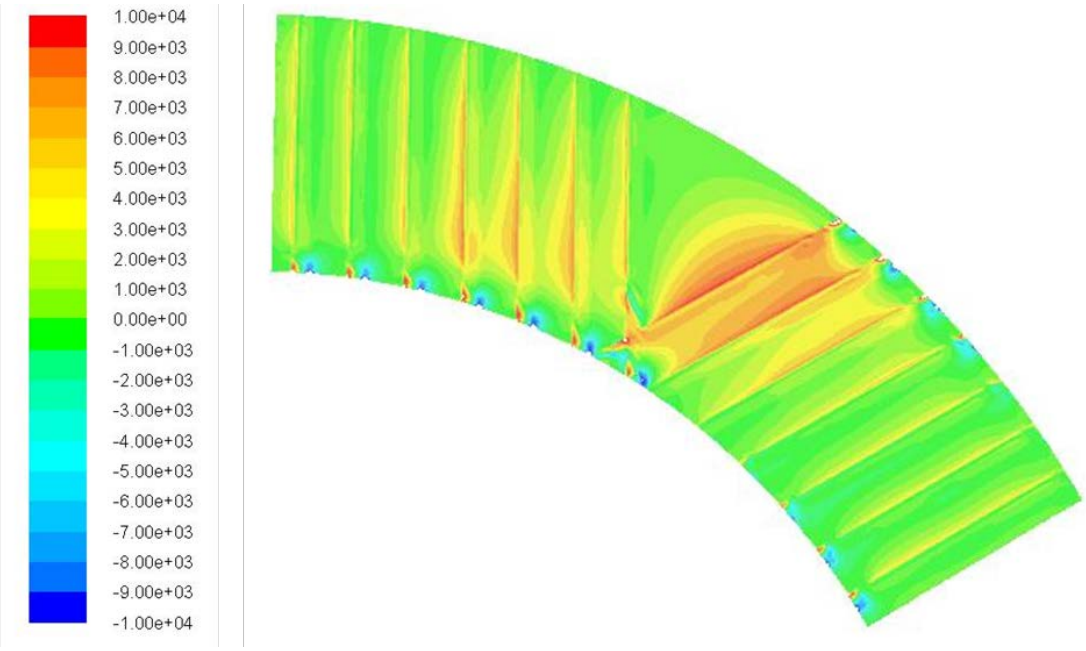

Figure 2: Pressure distribution (gauge) over the brake geometry determined through CFD

Figure 2 shows that near the inlet region at the inner radius of the disc, there are low pressure regions suggesting that cavitation may occur. Note that the CFD model used is a single phase analysis which only accounts for the fluid film lubrication. These results occur in regions where the film pressure drops below the ambient pressure, but any liberated gasses from the lubricant are not accounted for in order to normalise the pressure, whilst maintaining mass conservation. The central region of the contact and most of the modelled contact area appear to follow typical hydrodynamic behaviour showing increased pressure where there is converging geometry, dropping back to near atmospheric conditions in any divergent gap. There are clearly pressure perturbations at the leading edges of groove features. This effect is often referred to as micro-hydrodynamics, which can improve load carrying capacity of the contact, although their introduction in this case is not because of this purpose, but for convection of heat away when the discs are engaged to transmit power. Micro-hydrodynamic lift effect is intentionally introduced through surface texturing in contacts with poor contact kinematics (low value of U) or inlet wedge shape to promote lubrication via lubricant entrapment and micro-wedge effect [6, 7]. This opportunity may lend itself in this application as well, but it should be considered in thermos-hydrodynamics of engaged brake plates as heat transfer should not be unduly compromised.

However, the pressure variations affect the lubricant flow and viscous sear of the lubricant and thus the generated friction which is the primary interest of this study.

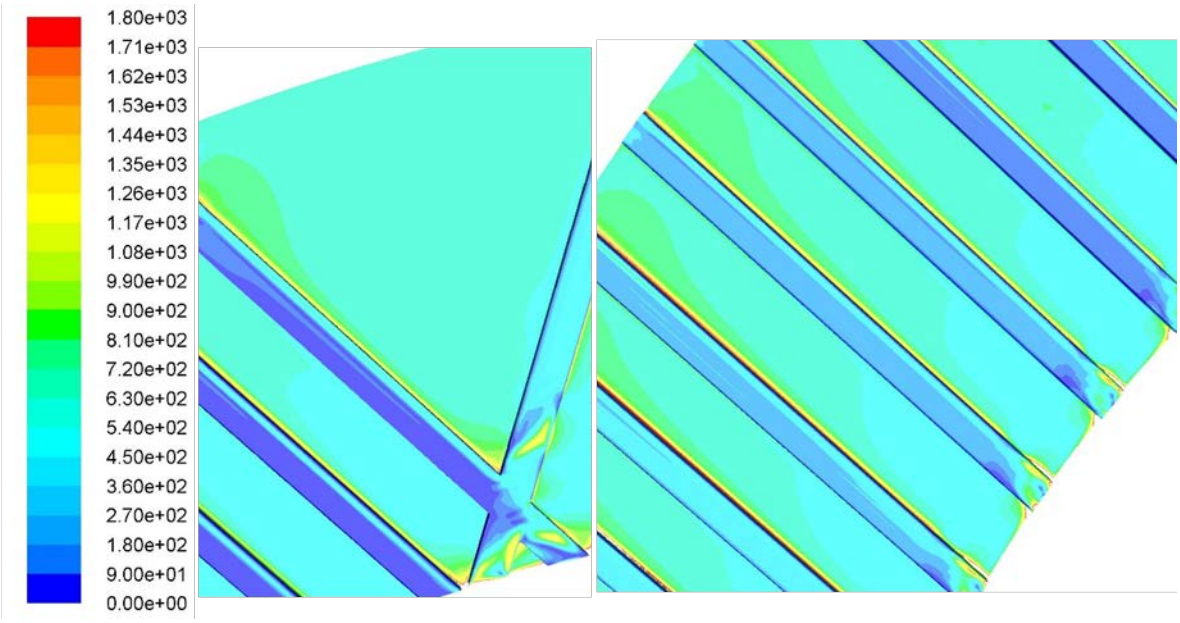

Figure 3: Viscous shear stress distribution over the brake geometry determined through CFD

Figure 3 shows that there is significant local variation in lubricant shear in the regions where there is a high pressure gradient. This includes the effect of pressure perturbations caused at the edges of the fabricated grooves. The torque predicted for the total brake interface losses for a single interface between a friction plate and its counter flat plate through CFD is 1.888 Nm.

5 – Predictions of the numerical Reynolds-based Model Results

The developed Reynolds-based model with inertial effect is applied to the same operational conditions (Table 1). The resultant pressure distribution is shown in Figure 4, in which the polar coordinate system is used.

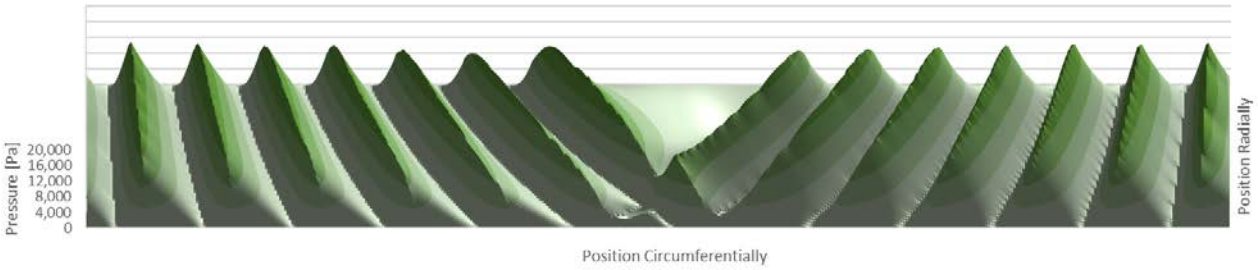

Figure 4: Pressure distribution in a repeated section of the brake disc conjunction

A comparison of Figures 2 and 4 shows that the predictions with the developed Reynolds-based model conform well with those of the more general, but computationally time-intensive CFD. There is a notable difference near the inlet of the inner radius of the disc, where the CFD predicts negative gauge pressure due to cavitation. The numerical model applies a Reynolds cavitation and reformation model, thus replacing any negative pressure in any cavitated region to the atmospheric pressure, thus the reason for this observed difference.

The predicted torque with the Reynolds-based numerical model is 1.8344 Nm (a power loss of 177.883 W at 926 rpm) for each interface between a rotating brake disc and its stationary counter plate. This prediction is within 3% of the torque predicted through CFD analysis.

6 – Experimental Investigation

In order to establish the validity of the numerical model as well as seek a combined numerical-experimental study of underlying mechanisms responsible for power loss, a component level test rig is developed with torque, rotational speed and temperature control. The rig (Figure 5) is designed such that a single brake friction plate can be rotated between two stationary counter plates at a controlled separation and rotational speed. The assembly is positioned in a heated bath of oil. In situ conditions are monitored with a torque and rotational speed transducer,simultaneously monitoring the system performance.

The combined torque and speed sensor used is a Torqsense RWT421-EC-KG with a sampling rate of 450 Hz, a sensitivity of ±0.05 Nm, an operational torque range of 0-50 Nm and an operational rotational speed range of 0-15000 rpm. Data acquisition is carried out with the Torqview software.

The test rig comprises a motor-driven, twin-pulley system to rotate a shaft connecting the motor to the rotor being tested via the torque transducer and a torque limiting coupling (set to a cut-off at 50 Nm to protect the torque transducer from any damage through overloading). A soft coupling connects the transducer to the input shaft to allow for any minor misalignments. The driven shaft rotates in a custom-built oil tank housing with deep grove ball bearings at its either end, locked against the housing with an end cap and a locking plate. The stator counter plates were separated by fixed spacers at 3 clamping points, but allowed to float and find an equilibrium position through hydrodynamic generated pressure.

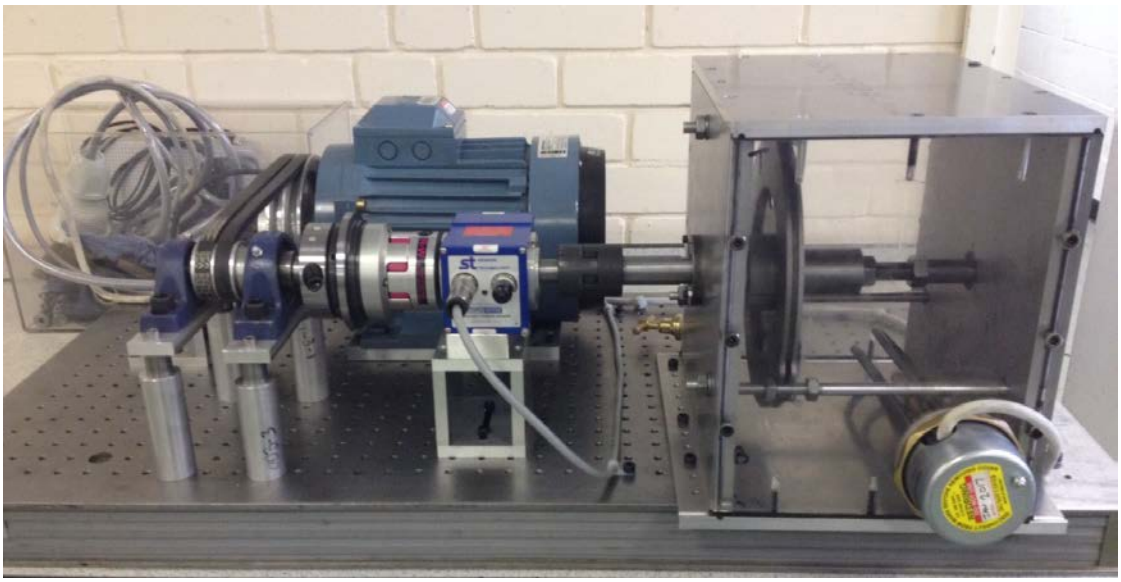

Figure 5: The component-level test rig

In order to isolate the torque of the tested rotating plate from the resistance of supporting bearings and shaft, the resistive torque of the rig without the drag of the brake-assembly is recorded first. As a result, the torque meter is initialised before the full test rig is run without oil at approximately 500 rpm for 10 minutes in order to ensure the bearings had reached thermal equilibrium conditions. Resistive torque measurements are then undertaken whilst varying the rotational speed up to the speed of 1000 rpm in order to obtain the baseline measurements without the contribution of the brake discs' conjunctions.

The oil tank is then filled to a level which submerges the friction plate to the level of its inner radius at its lowest positon and torque measurements are obtained at various oil temperatures. By subtracting the baseline torque from the total measured torque, including the contribution the

rotating brake plate between the two stator counter plates, the conjunctional frictional torque is determined.

7 – Experimental Validation

The rotational speeds, oil bath temperatures and separation of counter face discs are altered in a manner that the measurements replicate the input conditions to the developed numerical models for comparative purposes. The results of the comparisons are shown in Figure 6.

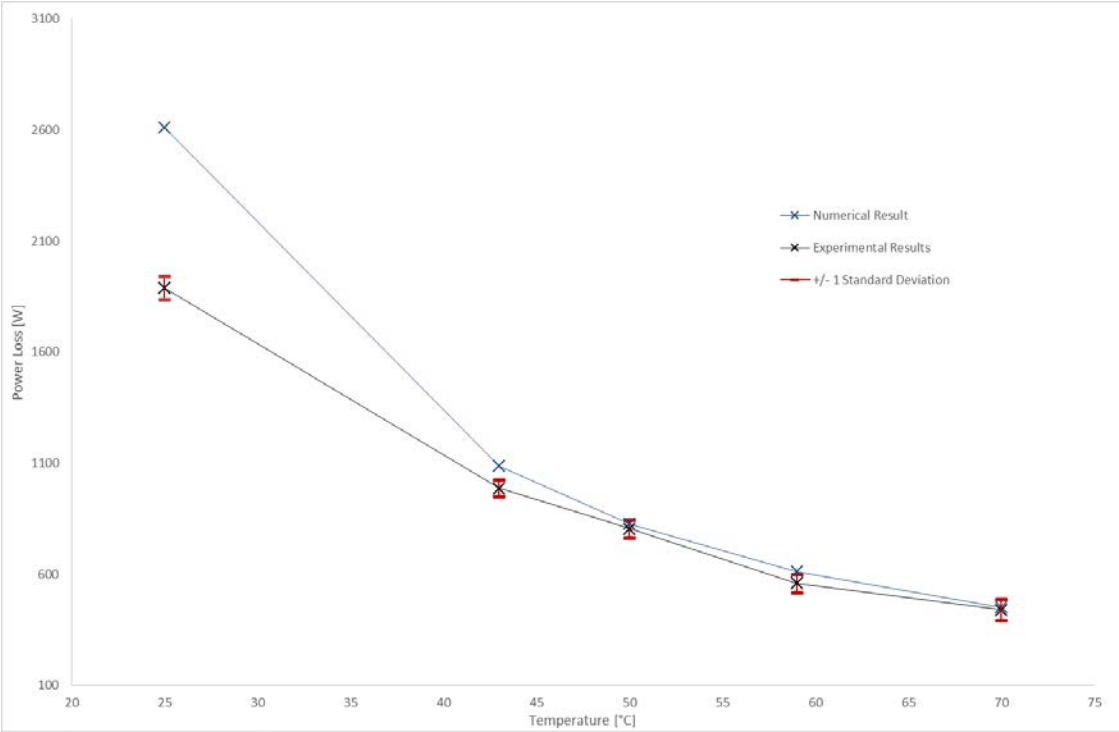

Figure 6: Comparison of experimental and numerical results for power loss of the brake system

It can be seen that at higher temperatures (thus lower lubricant viscosity) there is close agreement between the experimental and numerical results. There is significant variation found between the results at the lowest temperature. Visual observation of the experimental conditions indicate that at high rotational speeds with high lubricant viscosities at lower temperatures there is insufficient lubricant entrainment into the contact, causing inlet starvation. It should be noted that the numerical model assumes a fully flooded inlet. Also, detailed inlet boundary flow conditions into all forms of contact indicate some swirl and counter flow at the inlet conjunction, with only a

portion of the flow entering the contact after a stagnation point is reached (zero reverse flow boundary) [8-10]. Therefore, a more complex inlet flow dynamics is required in the solution of Reynolds equation to further investigate the non-conformity of the predictions with the experimental measurements. This means that the developed model is more suitable for steady state running conditions at higher brake system operating temperatures. Of course during the process of engagement, not studied here, combined squeeze and shear of the lubricant occurs under transient conditions. A generic solution for this is provided for annular disc pairs of viscous coupling systems for all forms of lubricants, with Stokes micro-continuum theory coupled with Reynolds solution, with Newtonian viscous shear as a special case relevant to the current study [11].

8 – Concluding Remarks

A close agreement is found between the developed Reynolds-based numerical model and a CFD solution. This is further supported by experimental results obtained from an in-house developed component-level test rig. The analysis show the role of surface grooves which are primarily fabricated for heat transfer purposes from the mating surfaces under bake engagement. In this regard the effect of micro-hydrodynamic phenomenon is noted, which would improve load carrying capacity, thus reducing friction, particularly under brake engagement. It is concluded that a more comprehensive analysis can be carried out to optimise the groove geometry to simultaneously improve heat transfer as well as load carrying capacity. It is also noted with low bulk lubricant temperatures deviations occur between the numerical predictions and experimental measurements, possibly due to inlet boundary starvation. It is proposed that more realistic boundary conditions than an assumed fully flooded inlet needs to be incorporated in the analysis. Nevertheless, very good agreement is obtained for the investigated cases with high lubricant bulk temperature.

Acknowledgements

The authors wish to express their gratitude to J. C. Bamford Excavators and the Innovate UK for their support of this project.

References

[1]- Cameron, A., “Basic Lubrication Theory”, Ellis Horwood Ltd., UK, 1981.

[2]- Gohar, R. and Rahnejat, H., “Fundamentals of Tribology”, Imperial College Press, London, 2008.

[3]-Gohar, R. and Safa, M., "Fluid film lubrication", In: Tribology and Dynamics of Engine and Powertrain, Woodhead Publications, 2010, pp. 132-170.

[4]- Razzaque, M. M. and Kato, T., “Effects of groove orientation on hydrodynamic behaviour of wet clutch coolant films”, Trans ASME, J. Tribology, 121(1), 1999, pp. 56-61.

[5]- Cho, J., Katopodes, N., Kapas, N. and Fujii, Y., “CFD modelling of squeeze film flow in wet clutch”, SAE Technical Paper, No.: 2011-01-1236, 2011.

[6]- Morris, N., Leighton, M., De la Cruz, M., Rahmani, R., Rahnejat, H. and Howell-Smith, S., “Combined numerical and experimental investigation of the micro-hydrodynamics of chevron-based textured patterns influencing conjunctional friction of sliding contacts”, Proc. IMechE, Part J: J. Engineering Tribology, 2015, 229(4), pp. 316-335

[7]- Etsion I., “Surface texturing for in-cylinder friction reduction”, New Delhi (India): Woodhead Publishing Ltd, 2010

[8]- Tipei, N., “Boundary conditions of a viscous flow between surfaces with rolling and sliding motion”, Trans. ASME, J. Lubn. Tech., 1968, 90(1), pp. 8–16

[9]- Mohammadpour, M., Johns-Rahnejat, P.M., Rahnejat, H. and Gohar, R., “Boundary conditions for elastohydrodynamics of circular point contacts”, Tribology Letters. 2014, 53(1), pp. 107-118.

[10]- Shahmohamadi, H., Mohammadpour, M., Rahmani, R., Rahnejat, H., Garner, C.P. and Howell-Smith, S., “On the boundary conditions in multi-phase flow through the piston ring-cylinder liner conjunction”, Tribology International, 2015, 90, pp. 164-174

[11]- Daliri, M., Jalali-Vahid, D. and Rahnejat, H., “Magneto-hydrodynamics of couple stress lubricants in combined squeeze and shear in parallel annular disc viscous coupling systems”, Proc. IMechE, Part J: J. Engineering Tribology, 2015, 229(5), 578-596